6-3-2011

Modeling nitrogen loadings from agricultural soils in southwest China with modified DNDC

Jia Deng
University of New Hampshire, Durham, Jia.Deng@unh.edu

Bo Zhu
Chinese Academy of Sciences

Zaixing Zhou
Chinese Academy of Sciences

Xunhua Zheng
Chinese Academy of Sciences

Changsheng Li
University of New Hampshire, Durham

See next page for additional authors

Recommended Citation

J. Deng, B. Zhu, Z. Zhou, X. Zheng, C. Li, T. Wang, J. Tang, 2011, Modeling Nitrogen Loadings from Agricultural Soils in Southwest China with Modified DNDC, Journal of Geophysical Research - biogeosciences, 116, G02020, doi:10.1029/2010JG001609.

Authors
Jia Deng, Bo Zhu, Zaixing Zhou, Xunhua Zheng, Changsheng Li, Tao Wang, and Jialiang Tang

Modeling nitrogen loadings from agricultural soils in southwest China with modified DNDC

Jia Deng,[1] Bo Zhu,[2] Zaixing Zhou,[1] Xunhua Zheng,[1] Changsheng Li,[3] Tao Wang,[2] and Jialiang Tang[2]

Received 11 November 2010; revised 22 February 2011; accepted 7 March 2011; published 3 June 2011.

[1] Degradation of water quality has been widely observed in China, and loadings of nitrogen (N) and other nutrients from agricultural systems play a key role in the water contamination. Process-based biogeochemical models have been applied to quantify nutrient loading from nonpoint sources at the watershed scale. However, this effort is often hindered by the fact that few existing biogeochemical models of nutrient cycling are able to simulate the two-dimensional soil hydrology. To overcome this challenge, we launched a new attempt to incorporate two fundamental hydrologic features, the Soil Conservation Service curve and the Modified Universal Soil Loss Equation functions, into a biogeochemistry model, Denitrification-Decomposition (DNDC). These two features have been widely utilized to quantify surface runoff and soil erosion in a suite of hydrologic models. We incorporated these features in the DNDC model to allow the biogeochemical and hydrologic processes to exchange data at a daily time step. By including the new features, DNDC gained the additional ability to simulate both horizontal and vertical movements of water and nutrients. The revised DNDC was tested against data sets observed in a small watershed dominated by farmlands in a mountainous area of southwest China. The modeled surface runoff flow, subsurface drainage flow, sediment yield, and N loading were in agreement with observations. To further observe the behaviors of the new model, we conducted a sensitivity test with varied climate, soil, and management conditions. The results indicated that precipitation was the most sensitive factor determining the rate of N loading from the tested site. A Monte Carlo test was conducted to quantify the potential uncertainty derived by variations in four selected input parameters. This study demonstrates that it is feasible and effective to use enhanced biogeochemical models such as DNDC for quantifying N loadings by incorporating basic hydrological features into the model framework.

Citation: Deng, J., B. Zhu, Z. Zhou, X. Zheng, C. Li, T. Wang, and J. Tang (2011), Modeling nitrogen loadings from agricultural soils in southwest China with modified DNDC, *J. Geophys. Res.*, *116*, G02020, doi:10.1029/2010JG001609.

1. Introduction

[2] Since the Green Revolution in the late 1950s, synthetic fertilizers have played a key role in sustaining ever-growing agricultural production. However, low fertilizer use efficiency results in a significant portion of the nutrients being transferred into bodies of water worldwide [*Carpenter et al.*, 1998; *Galloway et al.*, 2003; *Karlen*, 1998; *Tilman et al.*, 2001]. For instance, *Seitzinger et al.* [2005] estimated that about 25 Tg of dissolved inorganic nitrogen (N) was exported by rivers on a global scale, of which about 21% resulted directly from synthetic fertilizer use. In China, about 7% of the applied fertilizer N (about 1.8 Tg N) was estimated to have entered bodies of water in 2004 [*Z. Zhu et al.*, 2006]. Nonpoint (diffuse) source N pollution has been recognized as a primary source of eutrophication and groundwater contamination in many countries [*Novotny and Olem*, 1994; *Rabalais*, 2002; *Seitzinger*, 2008]. The loadings of N from soil into water systems result from the interaction between water movements and N transformation in the soil matrix [*Neitsch et al.*, 2001]. A large number of experiments conducted in the field and in laboratories have demonstrated the complex relationship between N loading and its drivers (e.g., climate, soil texture, crop phenology, farming management) [*Cassman et al.*, 2002; *Jaynes et al.*, 2001].

[3] During the past 2 decades, two kinds of modeling approaches have been applied to predict nutrient loadings. On

[1]State Key Laboratory of Atmospheric Boundary Layer Physics and Atmospheric Chemistry, Institute of Atmospheric Physics, Chinese Academy of Sciences, Beijing, China.

[2]Institute of Mountain Hazards and Environment, Chinese Academy of Sciences, Chengdu, China.

[3]Complex Systems Research Center, Institute for the Study of Earth, Oceans, and Space, University of New Hampshire, Durham, New Hampshire, USA.

0148-0227/11/2010JG001609

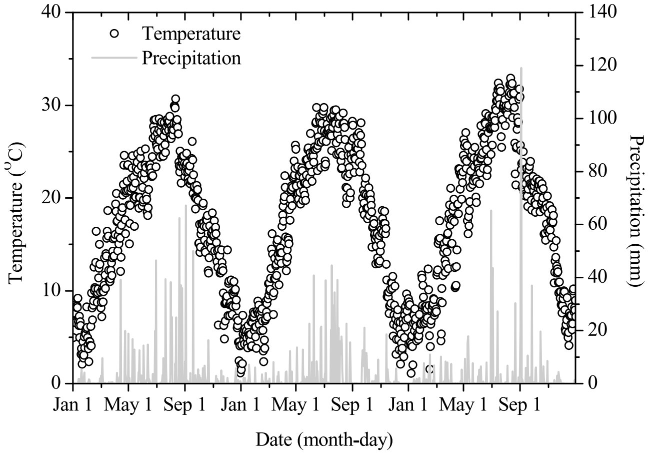

Figure 1. Daily average air temperature and precipitation during 2004–2006 at the experimental site in Yanting Agro-Ecological Station, Sichuan, China.

the one hand, a number of hydrologic models, such as MIKE SHE [*Refsgaard and Storm*, 1995], RHESSys [*Band et al.*, 2001; *Tague and Band*, 2004], and SWAT [*Arnold et al.*, 1998; *Neitsch et al.*, 2001; *Saleh et al.*, 2000], have been enhanced by incorporating nutrient transport and transformation into the model frameworks. On the other hand, several soil biogeochemical models have been modified by including more accurate hydrologic processes. For example, a process-based model of carbon (C) and N biogeochemistry, Denitrification-Decomposition or DNDC, has been modified to simulate N leaching losses with improved drainage algorithms [*Li et al.*, 2006; *Tonitto et al.*, 2007, 2010]. However, both approaches based upon hydrology- or biogeochemistry-oriented models have their advantages and disadvantages. The hydrologic models incorporate spatial distribution algorithms for simulating water movement at the watershed scale but usually lack detailed biogeochemical processes for nutrient transformation. In contrast, the biogeochemical models have relatively detailed processes for nutrient transformation but are unable to account for the transport of nutrients through lateral flow. Some researchers have tried to link the existing hydrologic and biogeochemical models to let them exchange input/output parameters [*Cui et al.*, 2005]. However, this approach was time-demanding and led to clumsy information feedback between hydrologic and biogeochemical models. As water flow and N transformation jointly control N loading in soils, it would be ideal to integrate the hydrologic process and detailed nutrient biogeochemistry into a single model framework. However, few existing models meet the criteria, considering the absence or simplified representation of complex processes of water or nutrient transformation in these models [e.g., *Boyer et al.*, 2006; *Kimura et al.*, 2009; *Li et al.*, 2006]. In this study, we undertook a new attempt to incorporate two fundamental hydrological features, the Soil Conservation Service (SCS) curve and the Modified Universal Soil Loss Equation (MUSLE) functions, into a biogeochemistry model, DNDC. These two features have been widely utilized to quantify surface runoff and soil erosion in a suite of hydrologic models. Here we report the modified DNDC and the applicability of the new model against field data sets observed in cropland in a small watershed in southwest China.

2. Field Site Description

[4] The Yanting Agro-Ecological Station (N31°16′, E105°28′, 400–600 m above sea level) is located in a hilly area of Sichuan Basin in southwest China. The area experiences a subtropical monsoon climate, with an annual mean temperature of 17.3°C and precipitation of 826 mm during 1981–2006. The local soil is classified as Pup-Orthic Entisol in the Chinese Soil Taxonomy, or an Entisol in the U.S. Soil Taxonomy [*Zhu et al.*, 2009]. The soil has pH of 8.3, bulk density of 1.33 g cm^{-3}, organic matter content of 8.75 g kg^{-1}, and saturated hydraulic conductivity of 0.28 mm min^{-1} [*Zhu et al.*, 2009]. Lysimeters (8 m × 4 m) with various slopes were permanently installed in the fields to measure surface runoff and subsurface drainage leaching flows starting in 2001. The cropping systems, fertilization, and other farming management practices at the lysimeter plots were consistent with the management commonly applied in the area. Winter wheat-summer maize rotation was adopted during the experimental period from 2004 to 2006. Each of the wheat seasons received 130 kg N ha^{-1} (as ammonia bicarbonate), 90 kg P_2O_5 ha^{-1} and 36 kg K_2O ha^{-1}. Each of the corn seasons received the same amounts of P_2O_5 and K_2O but 20 kg N ha^{-1}. The fertilizers were applied basally at the beginning of the crop season.

[5] During 2004–2006, field measurements were conducted at three replicate lysimeter plots in the Station. Each plot has an area of 32 m^2 with slope of 7°. The soil profile depth is 60 cm. The measured items included (1) surface runoff flow, (2) subsurface leaching flow, (3) sediment yield, (4) particulate and dissolved N concentrations in the surface runoff flow, (5) subsurface nitrate leaching flux, and (6) crop yield. Daily and annual water and N fluxes for the surface runoff and subsurface drainage flow were calculated based on the measurements of the tested plots [*Zhu et al.*, 2008, 2009]. The technical details of the field experiments have been described by *Zhu et al.* [2009].

[6] During the experimental period, the annual precipitation was 860, 835, and 806 mm for 2004, 2005, and 2006, respectively, mainly occurring from May to October (Figure 1) [*Zhu et al.*, 2009]. Measurements indicated that (1) rainfall events resulted in significant surface runoff and subsurface drainage flow from May through October, (2) about 15% of N fertilizer was lost through the surface runoff and subsurface drainage flow, and (3) the N losses were highly variable in time, driven by weather, soil, and farming management conditions [*Wang et al.*, 2006; *B. Zhu et al.*, 2006; *Zhu et al.*, 2008, 2009]. The 3 year measurements provide a unique data set containing synchronized water and N fluxes from both surface runoff and subsurface drainage for a same site. This data set was used to test the modified DNDC in the study.

3. Model Modifications

[7] We hypothesized that the capacity of a biogeochemistry model for simulating N loadings could be improved if the basic hydrological algorithms were incorporated into the model framework. The DNDC model was adopted to test this hypothesis. DNDC was originally developed for quantifying

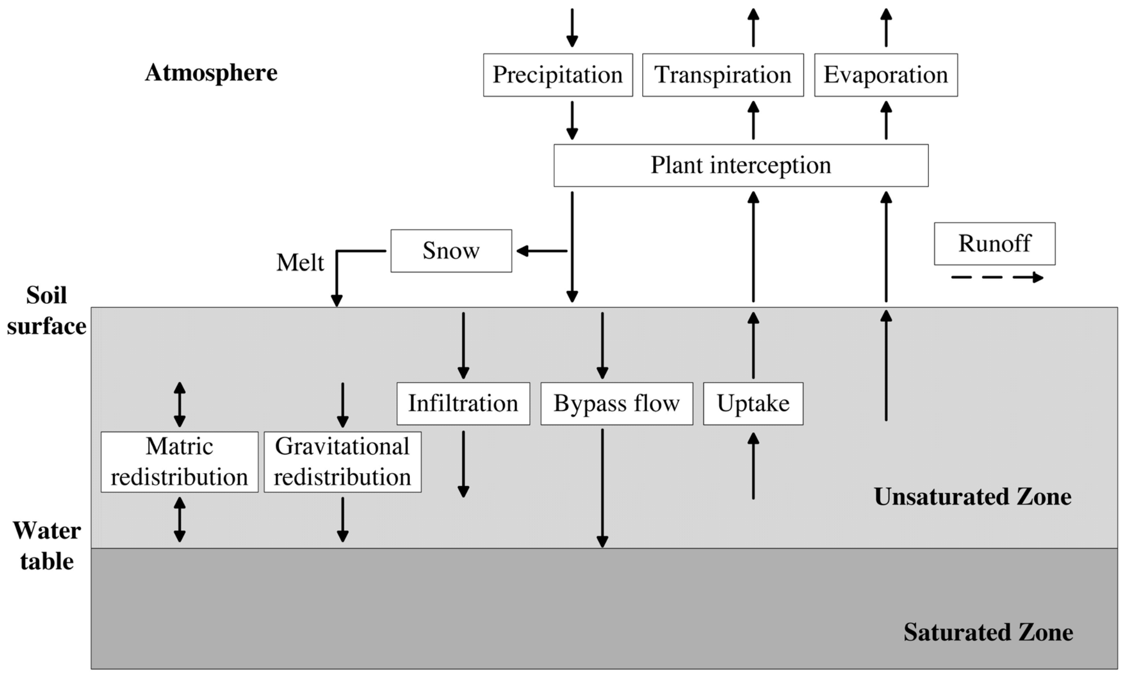

Figure 2. Structure of the soil hydrology submodel of DNDC. The solid arrows represent the processes originally existing in DNDC, and the dotted arrow represents the new process added to the model in this study.

carbon sequestration and greenhouse gas emissions from U.S. agricultural lands [*Li*, 2000; *Li et al.*, 1992a, 1992b, 1994, 1996]. A relatively complete suite of biochemical and geochemical processes (e.g., decomposition, nitrification, denitrification, ammonia volatilization, fermentation) has been embedded in the model, which enables it to precisely compute the complex transformations of C and N in agroecosystems. DNDC consists of two components. The first component consists of the soil climate, crop growth, and decomposition submodels that convert primary drivers (e.g., climate, soil properties, vegetation, and anthropogenic activity) to soil environmental factors (e.g., temperature, moisture, pH, redox potential, and substrate concentration gradients). The second component consists of the nitrification, denitrification, and fermentation submodels that simulate C and N transformations mediated by the soil microbial activities. In DNDC, soil N exists in several pools, including organic N, ammonium, ammonia, and nitrate. Nitrogen exchange between the pools is driven by a series of biogeochemical reactions, such as decomposition, nitrification, ammonia volatilization, ammonium adsorption, denitrification, and nitrate dissolution. DNDC tracks N dynamics and quantifies the sizes of the N pools in each layer of the soil profile at a daily or hourly time step. The original version of DNDC had routines calculating vertical water movement driven by precipitation, transpiration, evaporation, infiltration, and drainage [*Li et al.*, 2006; *Tonitto et al.*, 2007, 2010; *Zhang et al.*, 2002]. If drainage occurs in a soil layer, a fraction of the nitrate existing in the layer will be distributed into the leachate [*Li et al.*, 2006]. However, the original version of DNDC did not explicitly simulate surface runoff and was therefore unable to estimate sediment yield or nutrient transport associated with the surface runoff (Figure 2). This deficiency limited the applicability of DNDC for estimating N loadings from watersheds. To improve the model's performance, we incorporated the SCS curve and the MUSLE functions into the framework of DNDC.

[8] The SCS curve [*Mockus*, 1972; *Williams*, 1995] has been widely utilized in hydrologic models. By using an empirical number, the Curve Number or CN, the SCS function calculates surface runoff flow based on precipitations and several soil hydrologic parameters shown as follows:

$$\begin{aligned} Q &= (P - Ia)^2/(P + S - Ia) \quad \text{if} \quad P > Ia \\ Q &= 0 \quad \text{if} \quad P \leq Ia \end{aligned} \tag{1}$$

where Q is daily surface runoff (mm H_2O), P is daily precipitation (mm H_2O), Ia is the initial water abstraction (the value accumulated precipitation must exceed before surface runoff occurs), and S is the soil water retention parameter (mm H_2O).

[9] The retention parameter (S) is related to the Curve Number (CN) according to SCS equation [*Mockus*, 1972]:

$$S = 25400/CN - 254 \tag{2}$$

[10] During the model simulation, the value of S is updated at a daily time step based on soil water content shown as follows [*Neitsch et al.*, 2001; *Williams*, 1995]:

$$S = S_{\max} \cdot \{1 - SW/[SW + \exp(w_1 - w_2 \cdot SW)]\} \tag{3}$$

where S is daily retention parameter (mm H_2O), S_{max} is the maximum retention parameter on any given day (mm H_2O), SW is amount of water in soil profile (mm H_2O), and w_1, w_2 are shape coefficients. The parameter S_{max} is calculated by solving equation (2) using the curve number in dry moisture condition (CN_1); the CN_1 is determined based on the curve number in average moisture condition (CN_2) (see equation (A4) in Appendix A). The shape coefficients, w_1 and w_2, are calculated based on the retention parameters in the dry and moisture conditions (S_{max}, S_3) and several soil hydrologic parameters (see details in equations (A8) and (A9) in Appendix A). The value of CN_2 is usually obtained from a table based on the soil permeability and land use type or determined by calibration [*SCS*, 1986; *White and Chaubey*, 2005].

[11] Theoretically, the Ia value represents initial water losses due to the soil surface water storage, interception, and infiltration prior to the occurrence of surface runoff. The Ia value can be computed by measuring the amount of the rainfall during the period from the beginning of precipitation until the occurrence of the surface runoff. In practice, the Ia value is empirically determined as 0.2 S [*Neitsch et al.*, 2001].

[12] The Modified Universal Soil Loss Equation (MUSLE) [*Williams*, 1975, 1995; *Wischmeier and Smith*, 1978] calculates soil erosion based on the surface runoff flow and other soil surface properties specified as follows:

$$sed = 11.8 \cdot \left(q_{peak} \cdot Q \cdot A\right)^{0.56} \cdot K \cdot LS \cdot C \cdot P_S \cdot R \qquad (4)$$

where sed is sediment yield (metric ton soil d^{-1}), Q is surface runoff flow (mm d^{-1}), q_{peak} represents the peak runoff rate ($m^3\ s^{-1}$), A is the area of a plot or hydrology responsibility unit (ha), K is the soil erodibility factor, C is the soil surface cover and management factor, P_S is the factor related to soil conservation management practices, LS is the topographic factor, and R is the soil coarse fragment factor. The parameter q_{peak} is calculated based on rainfall intensity, surface runoff, time of concentration, etc. (see details in equations (A12)–(A16) in Appendix A). K can be determined by field measurement or calculated as a function of soil texture (see equations (A17)–(A21) in Appendix A); it was fixed as 0.4 in this study. C is a function of vegetation coverage, whose value was fixed as 0.25 in this study. Ps was set as 1. LS is a function of the slope and slope length (see equations (A22)–(A24) in Appendix A). R is calculated based on the stone fraction in the soil (see equation (A25) in Appendix A).

[13] Based on the MUSLE functions, the N losses from soil erosion can be calculated as described by *McElroy et al.* [1976] and *Williams and Hann* [1978]:

$$SedN = 0.001 conc_{sedN} \cdot sed/A \cdot \varepsilon_{sedN} \qquad (5)$$

where SedN is the sediment N loss with the surface runoff (kg N $ha^{-1}\ d^{-1}$), $conc_{sedN}$ is the concentration of sediment N in the surface soil (g N $tonne^{-1}$), sed is the runoff-induced sediment yield (metric ton soil d^{-1}), A is the area of the hydrology responsibility unit (ha), and ε_{sedN} is the N enrichment ratio (see details in equations (A26)–(A28)) in Appendix A).

[14] The above described SCS curve and MUSLE functions have been incorporated in DNDC at code level so that the revised DNDC can simulates both the water flow and N biogeochemistry in synchrony at daily time step. The modifications have substantially improved the capacity of the DNDC for modeling the soil N losses through both surface runoff and subsurface drainage flows. This two-dimensional simulating ability should have set a sound basis for the model to be applied at watershed scale.

4. Model Tests

[15] To confirm the applicability of the modified DNDC, we conducted tests against the observed data sets of crop yield, surface runoff flow, subsurface drainage flow, sediment yield, and N losses at the experimental site. Because the revised DNDC contains the SCS and MUSLE functions, several new input parameters were required to run the model, including the plot slope, slope length, plot surface area, initial CN value, soil erodibility factor (K), soil surface cover and management factor (C), and soil conservation management factor (Ps). In this study, the values of plot slope, slope length, and plot surface area were 7°, 8 m, and 32 m^2, respectively, based on the field measurement. The bounds of initial CN, K, and C (73–83, 0.33–0.45, and 0.20–0.30, respectively) were set by referring to other studies with similar soil, hydrologic conditions, and managements [*Deng et al.*, 2003; *Gao et al.*, 2006; *Neitsch et al.*, 2001; *SCS*, 1986; *Shi et al.*, 1997; *Wischmeier and Smith*, 1978; *Zhang et al.*, 2001]. Through calibration with 2004 field data, the values of initial CN, K, and C were fixed as 77, 0.40, and 0.25, respectively. The P value was set as 1.0, as no specific soil conservation management practices (e.g., contour tillage, contour strip cropping or terrace land reforming) took place in the experimental field. The daily maximum 0.5 h rainfall was determined based on detailed weather records. The rate of bypass flow through the soil macropores was 0.2 based on observed subsurface leaching flow in 2004. In general, the data measured in 2004 were utilized to calibrate the input parameters described above, and the data from 2005 and 2006 were used for model validation.

[16] The revised DNDC was run for 2005 and 2006, and the modeled results were compared with observations of crop yield, surface runoff flow, subsurface drainage flow, sediment yield, and N losses with surface runoff or subsurface drainage flow. Two statistical indexes, the Nash-Sutcliffe index of model efficiency (ME) and the coefficient of determination (R^2), were used for quantitative comparisons. ME is a measure of improvement in prediction as compared to the mean of observations (equation (6)). A positive ME value indicates that the model prediction is better than the mean of observations, and the best model performance has ME value equal to 1 [*Miehle et al.*, 2006; *Nash and Sutcliffe*, 1970]. The coefficient of determination (R^2) examines the correlation between model predictions and field observations (equation (7)).

$$ME = 1 - \frac{\sum_{i=1}^{n} (p_i - o_i)^2}{\sum_{i=1}^{n} (o_i - \overline{o})^2} \qquad (6)$$

$$R^2 = \left(\frac{\sum_{i=1}^{n} (o_i - \overline{o})(p_i - \overline{p})}{\sqrt{\sum_{i=1}^{n} (o_i - \overline{o})^2 \sum_{i=1}^{n} (p_i - \overline{p})^2}} \right)^2 \qquad (7)$$

where o_i and p_i are the observed and simulated values, $\overline{o}$ and $\overline{p}$ are their averages and n is the number of values.

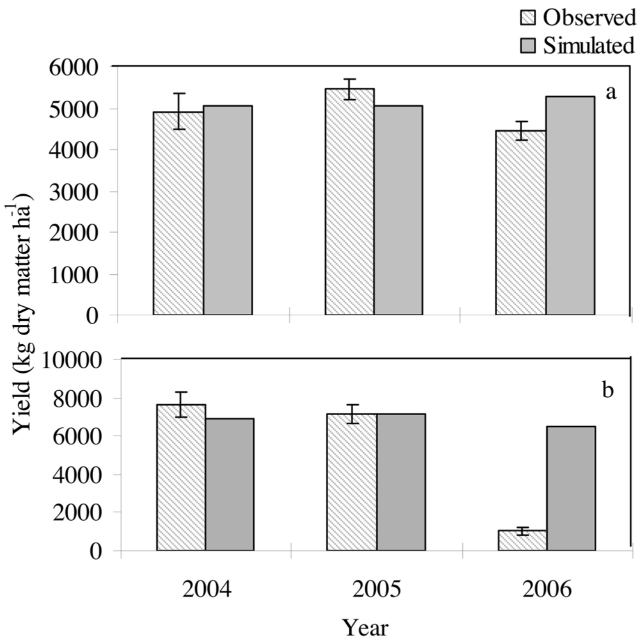

Figure 3. Comparisons between simulated and observed yields of (a) winter wheat and (b) maize planted in the experimental field. Observed yields are the mean values of three replicates. The vertical bars represent standard errors.

4.1. Comparison Between Observed and Modeled Crop Yields

[17] In agroecosystems, crop growth plays a key role in determining the soil environment and nutrient status. Correctly simulating the crop growth is a precondition for modeling soil biogeochemical processes. The revised DNDC was run for 3 years (2004–2006) based on the actual climate, soil, and farming management conditions at the experimental site. The modeled yields of wheat and maize are in agreement with observations for all of the seasons, except for maize in 2006 (Figure 3). In 2006, maize growth was depressed by a short-term drought occurring in the crop jointing stage in the experimental field; DNDC missed the impact of the short-term drought. Except for this single season, the modeled yields deviated from the observations by 7.7% on average (ranging from 0.4% to 18.7%).

4.2. Comparison Between Observed and Modeled Surface Runoff and Subsurface Drainage Flows

[18] Observed surface runoff and subsurface drainage flow showed a clear relationship with the rainfall events in the experimental field. Driven by the local weather data, soil properties, and farming management practices, DNDC produced daily surface runoff and subsurface drainage flows for 2005 and 2006. The modeled daily surface runoff flow during the rainfall events ranged from 2.5 to 98.2 mm, with a mean of 18.1 mm. The results are comparable to observed measurements, ranging from 4.6 to 83.8 mm with a mean of 18.1 mm. The patterns of the modeled surface runoff flows also match observations (Figure 4a). The correlation between the simulated and observed surface runoff is statistically significant ($R^2 = 0.99$, $p < 0.01$; ME = 0.95, Figure 5a). However, it may be noteworthy that interpreting the accuracy of simulated extreme surface runoff is difficult due to inadequate data availability (Figures 4a and 5a, 4 September 2006). The statistical result could be affected by the fact that measurements only include one extreme event [*Moriasi et al.*, 2007]. In spite of the single event on 4 September 2006, the correlation between the modeled and observed surface runoff is still high ($R^2 = 0.92$, $p < 0.01$).

[19] The simulated daily subsurface drainage flows during rainfall events ranged from 2.6 to 86.6 mm, with a mean of 19.0 mm. These results are in agreement with measurements ranging from 2.9 to 92.4 mm, with a mean of 19.5 mm. Figures 4b and 5b show that the patterns and magnitudes of the modeled and observed subsurface leaching fluxes have a significant correlation ($R^2 = 0.97$, $p < 0.01$; ME = 0.96). These results suggest that the revised DNDC is capable of simulating both the horizontal and vertical water flows in the tested field.

4.3. Comparison Between Observed and Modeled Sediment Yields

[20] The modeled daily sediment yields during rainfall events ranged from 219 to 11397 kg ha^{-1}, with a mean of 2107 kg ha^{-1}. These results are comparable with measurements ranging from 172 to 11818 kg ha^{-1}, with a mean of 2176 kg ha^{-1}. The model well captured the magnitudes and seasonal variations of the sediment yields compared with observations ($R^2 = 0.99$, $p < 0.01$; ME = 1.00) (Figures 4c and 5c). Similar to the surface runoff simulations, peak sediment yield predictions were highly uncertain due to inadequate observations during intensive storm events (Figure 5c).

4.4. Comparison Between Observed and Modeled Nitrogen Losses With Surface Runoff or Subsurface Leaching Flows

[21] DNDC calculates N losses with the surface runoff flow based on the organic and inorganic N contents in the eroded soils. The field measurements captured nine episodes of losses of particulate N, mainly in organic forms, driven by rainfall events during 2005 and 2006. The measured loss rates ranged from 0.03 to 7.96 kg N ha^{-1}, with a mean of 1.14 kg N ha^{-1}, while the modeled results ranged from 0.12 to 6.10 kg N ha^{-1}, with a mean of 0.92 kg N ha^{-1} (Figure 4d). Comparison between the modeled and measured particulate N losses gave a high ME value (0.93). Figure 5d demonstrated a significant zero-intercept linear regression of the modeled N losses against observations ($R^2 = 0.98$, $p < 0.01$). However, Figure 5d also shows that the model could underestimate particulate N losses by about 23% on average. The total N loss with the surface runoff flow is the sum of the losses of the N in both particulate and dissolved forms in the flow. The modeled daily total N losses varied between 0.18 and 8.20 kg N ha^{-1}, with a mean of 1.34 kg N ha^{-1}, a result that is similar to observations ranging from 0.18 to 8.29 kg N ha^{-1}, with a mean of 1.33 kg N ha^{-1} (Figure 4e). There is a significant zero-incept linear regression between the simulated and observed daily total N losses ($R^2 = 1.00$, $p < 0.01$; ME = 1.00). However, there was one measured flux on the high end that could skew the statistical result [*Moriasi et al.*, 2007]. By excluding the single high value

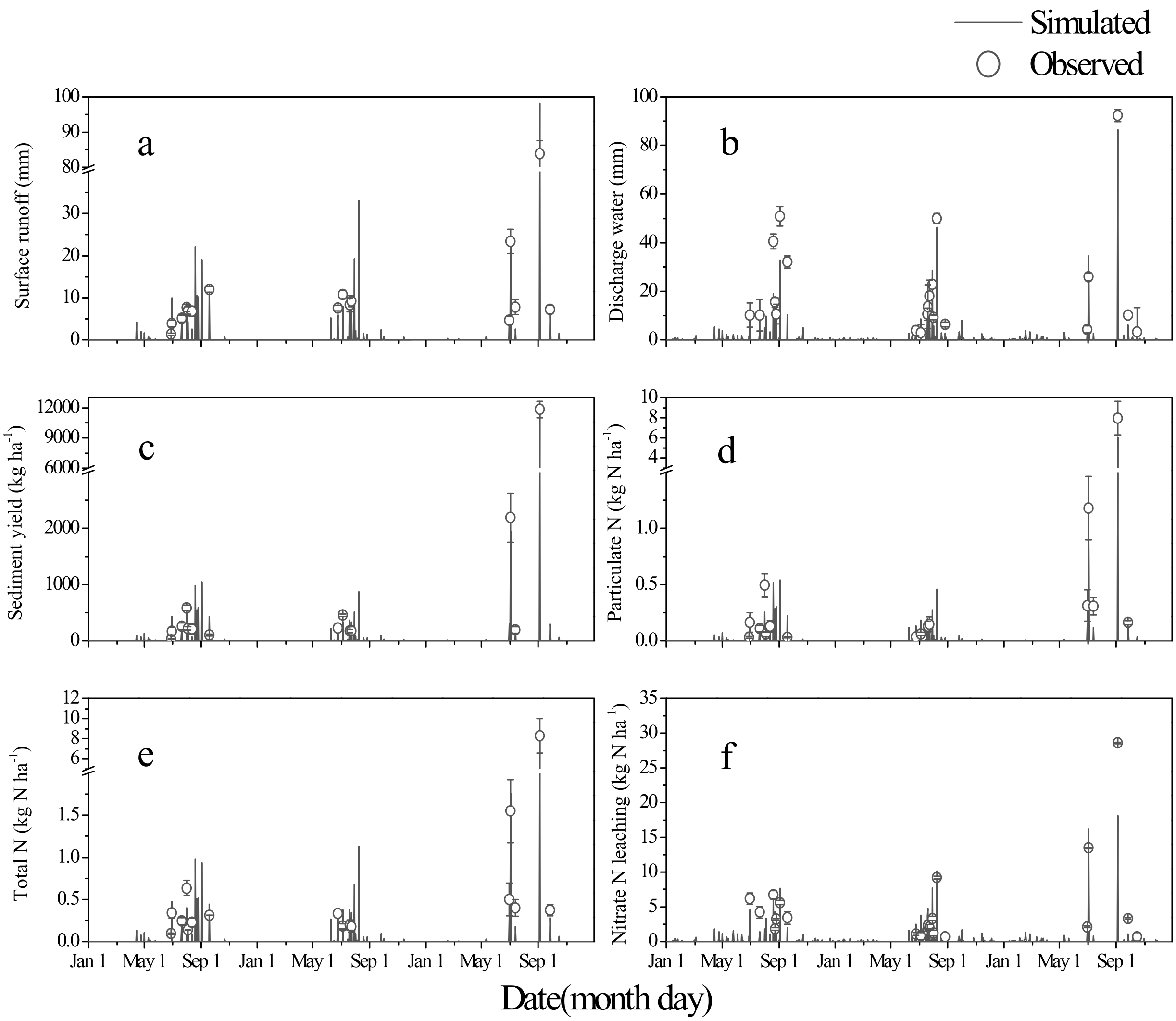

Figure 4. Simulated and observed (a) surface runoff flows, (b) subsurface drainage water flows, (c) sediment yields, (d) particulate nitrogen losses with surface runoff, (e) total nitrogen losses with surface runoff, and (f) nitrate leaching losses from 2004 to 2006. Observations are mean values of three replicates with standard error bars.

observed on 4 September 2006, we recalculated the R^2 and ME values. The new results still showed significant correlations between the measured and modeled particulate N losses (R^2 0.91 and ME 0.90) or total N losses (R^2 0.90 and ME 0.85).

[22] The original DNDC quantified nitrate leaching loss by simulating the vertical movement of water as well as the distribution of nitrate between liquid and solid phases in the soil profile [*Li et al.*, 2006]. The addition of the SCS and MUSLE functions improved the simulation of the subsurface drainage by more accurately estimating surface runoff flow based upon the water mass balance. In this study, the modeled daily nitrate leaching losses during the rainfall events ranged from 0.5 to 18.1 kg N ha^{-1}, with a mean of 5.4 kg N ha^{-1}. These results are comparable to observations ranging from 0.7 to 28.6 kg N ha^{-1}, with a mean of 5.1 kg N ha^{-1}. DNDC basically captured the seasonal pattern of nitrate losses through the subsurface drainage flow (Figures 4f and 5f). The correlation between the model outcomes and observations is statistically significant (R^2 = 0.95, $p < 0.01$; ME = 0.79), although the slope of 0.79 for the zero-intercept linear regression indicates that DNDC could have underestimated leached nitrate by about 20%.

[23] In summary, results from comparisons between the observed and modeled surface runoff flow, subsurface drainage flow, sediment yields, soil N losses, and crop yield indicate that the revised DNDC is capable of describing water, sediment, and N fluxes from an agricultural field with sloping terrain.

5. Sensitivity Analysis

[24] To investigate the general behaviors of the revised DNDC, we conducted a series of sensitivity tests by varying several input parameters including climate (precipitation), landform (slope), soil property (SOC), and management practice (fertilization). The baseline scenario was set based on the actual conditions at the experiment site in the Yanting

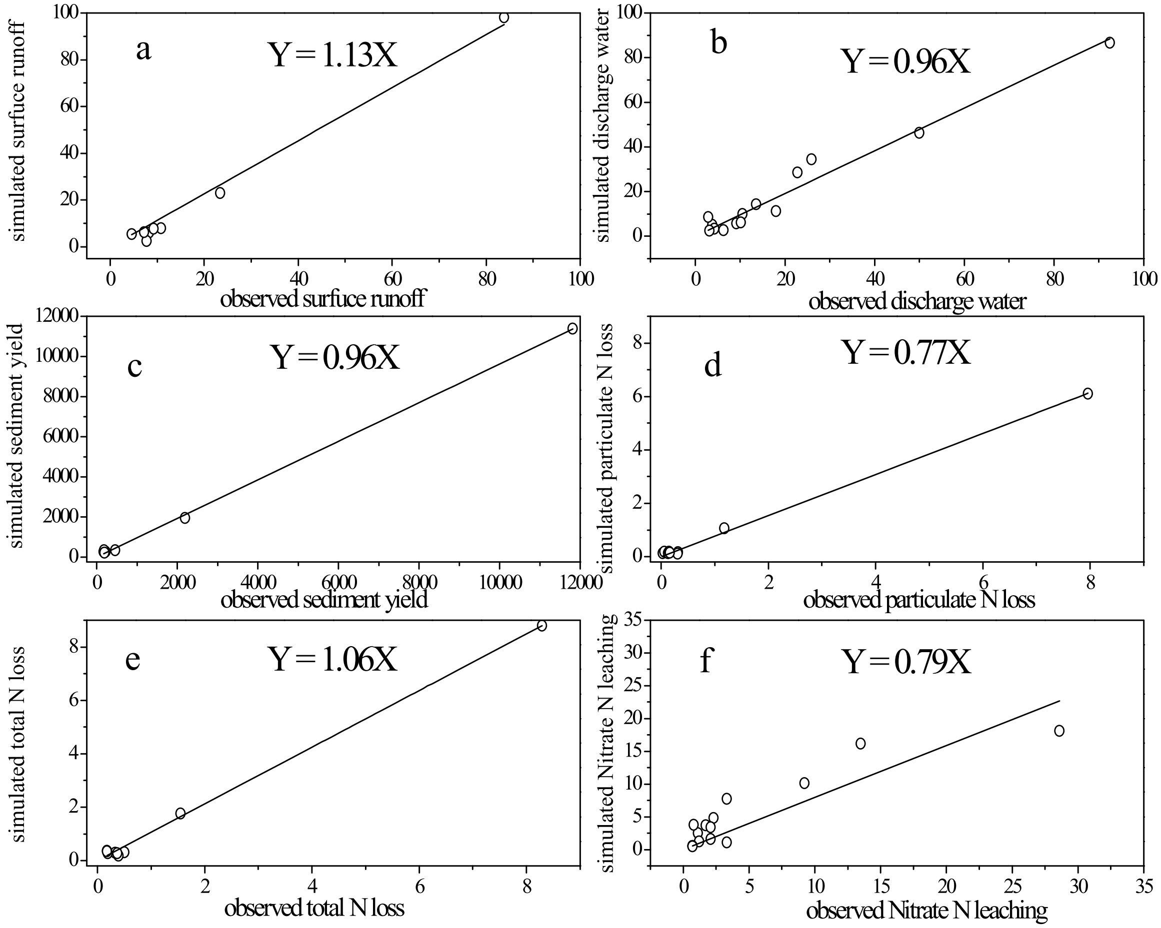

Figure 5. Comparisons between simulated and observed (a) surface runoff flow (mm), (b) subsurface drainage water flow (mm), (c) sediment yield (kg ha^{-1}), (d) particulate nitrogen loss with surface runoff (kg N ha^{-1}), (e) total nitrogen loss with surface runoff (kg N ha^{-1}), and (f) nitrate leaching loss (kg N ha^{-1}) during rainfall events in 2005 and 2006. The solid lines represent the zero-intercept linear regression. Observations are the mean values of three duplicates.

Agro-Ecological Station, which consists of land slope 7°, annual precipitation 860 mm, SOC content 5.0 g C kg^{-1} and nitrogenous fertilizer (ammonia bicarbonate) application rate 280 kg N ha^{-1} yr^{-1}. Daily climate data of 2005 were adopted for the baseline simulation. Alternative scenarios were created by varying a single input parameter while keeping others constants. The varied ranges were 1–13° for slope, 602–1118 mm for precipitation, 0.1–10 g C kg^{-1} for SOC content, and 196–364 kg N ha^{-1} for fertilizer application rate. The surface runoff flow, subsurface drainage flow, sediment yield, and N losses simulated with each of the scenarios were collected for comparison. The sensitivity of the modeled water, sediment or N fluxes to the input parameters was expressed with a sensitivity index (SI) following *Nearing et al.* [1990] and *Walker et al.* [2000]. The sensitivity index (SI) was calculated as follows:

$$SI = \left((O_2 - O_1)/O_{avg}\right)/\left((I_2 - I_1)/I_{avg}\right) \quad (8)$$

where I_1, I_2, and I_{avg} are the minimum, maximum, and average values of a selected input parameter, O_1, O_2, and O_{avg} are the corresponding modeled fluxes of water, sediment or N losses.

[25] The calculated SI values are shown in Table 1. The results indicated that (1) N losses through either surface runoff or subsurface drainage flow were very sensitive to variation in precipitation, which dominated almost all of the tested fluxes; (2) the variation in slope mainly affected the sediment yield and relevant particulate N loss; and (3) the variation in fertilizer application rate mainly affected N losses through subsurface drainage discharge. These results are in agreement with observations reported by other researchers [*Ng Kee Kwong et al.*, 2002; *Schlesinger et al.*, 1999] and imply that the revised DNDC has normal behaviors in simulating water, sediment, and N fluxes in the agroecosystems with sloping landforms.

6. Uncertainty Test

[26] When applying a model to predict soil N losses, a large uncertainty could result from the propagation of the uncertainties derived from the parameters employed either in the model structure or from input data. In this study, the

Table 1. Calculated Sensitivity Indices Quantifying the Impacts of Variations of Four Input Parameters on Water, Sediment, and N Fluxes Modeled With the Revised DNDC[a]

Tested Input Parameters			SI[b]					
Items	Baseline	Range	SR	SDW	SL	PN	TSN	NL
Precipitation (mm yr^{-1})	860	602–1118	2.19	2.13	2.08	2.07	2.13	1.78
Slope (°)	7	1–13	0.36	−0.17	1.11	1.11	0.85	−0.01
SOC content (kg C kg^{-1})	5	0.1–10	0.00	0.00	0.00	0.90	0.42	0.01
Fertilizer rate (kg N ha^{-1} yr^{-1})	280	196–364	0.00	0.00	0.00	0.09	0.15	1.52

[a]SR, surface runoff; SDW, subsurface drainage water; SL, sediment loading; PN, particulate nitrogen; TSN, total sediment nitrogen; NL, nitrate leaching.
[b]SI is the relative sensitivity index; the higher the absolute value of the S, the greater the impact the input has on the output.

soil hydrologic parameters such as initial CN, K, C, and bypass flow rate were required to support the SCS and MUSLE calculations. We empirically fixed the values of the parameters by calibration with field observations. This process could have produced errors in the parameter values. These errors will be eventually reflected in the modeled results through the model simulation. To quantify the potential uncertainty derived from the possible errors in the values of CN, K, C or bypass flow rate, we performed Monte Carlo simulations using the Latin Hypercube Sampling strategy [*Helton and Davis*, 2003]. As mentioned earlier, the initial values of CN, K, and C varied from 73 to 83, 0.33–0.45, and 0.20–0.30, respectively. We arbitrarily set the variation for bypass flow rate between ±25% of the value determined

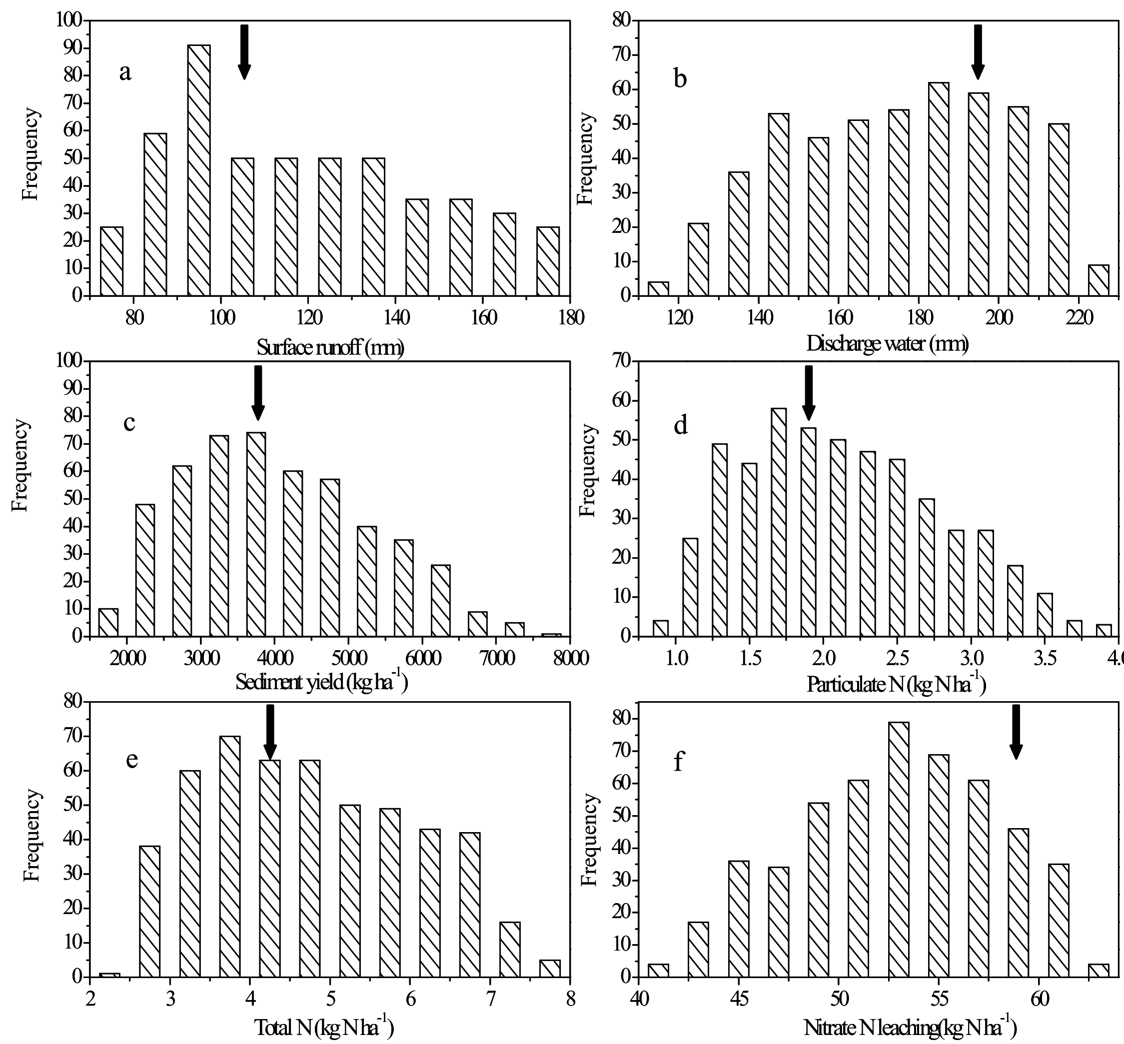

Figure 6. Frequency distributions of the (a) surface runoff flows, (b) subsurface drainage water flows, (c) sediment yields, (d) particulate nitrogen losses with surface runoff, (e) total nitrogen losses with surface runoff, and (f) nitrate leaching losses produced from 500 simulations in the Monte Carlo test. The solid arrows indicate the intervals where the baseline-simulated results fell.

Table 2. Variations and Means of Annual Water, Sediment, and N Flux Modeled With Revised DNDC in the Monte Carlo Test[a]

	SR	SDW	SL	PN	TSN	NL
Variation range from Monte Carlo test	74–175	118–222	1638–7522	0.87–3.99	2.45–7.98	40.5–62.7
Mean from Monte Carlo test	119	175	4028	2.14	4.76	52.8
Baseline-simulated result	108	200	3647	1.93	4.29	58.0
Difference between Monte Carlo mean and baseline result	11 (9%)	25 (14%)	381 (9%)	0.21 (10%)	0.47 (10%)	5.2 (10%)

[a]SR, surface runoff (mm); SDW, subsurface drainage water (mm); SL, sediment loading (kg ha^{-1} yr^{-1}); PN, particulate nitrogen (kg N ha^{-1} yr^{-1}); TSN, total sediment nitrogen (kg N ha^{-1} yr^{-1}); NL, nitrate leaching (kg N ha^{-1} yr^{-1}).

based on the field measurement. We assumed that the frequency distributions of all the parameters were uniform. In this study, simulation in 2005 was selected as the base scenario to illustrate the uncertainty derived from input variance.

[27] The initial values of CN, K, C, and bypass flow rate were randomly picked from the corresponding ranges to compose a scenario. Five hundred combination scenarios were then simulated in the Monte Carlo test. The Latin Hypercube Sampling strategy generated a distribution of plausible collections of parameter values from the multidimensional distribution. Frequencies of the modeled annual surface runoff flows, drainage water flows, sediment yields, particulate N losses, total surface N losses, and nitrate leaching losses resulting from the 500 simulations were calculated (Figure 6 and Table 2). The Monte Carlo test indicated that (1) the baseline-simulated results are located within the ranges derived from the Monte Carlo analysis; (2) possible variance of input parameters produced large uncertainty in modeled water, sediment, and N fluxes; and (3) the baseline results have a difference between 9 and 14% compared with the means across all Monte Carlo simulations (Table 2).

7. Discussion and Conclusion

[28] Contemporary agriculture is in state of transition, with more concern placed on ecosystem services. In China, especially southwest China where about 90% of agricultural lands are located in mountainous areas [*Yan et al.*, 2007], loadings of N from agricultural nonpoint sources threaten water quality at large scales [*Zhu et al.*, 2009]. Researchers, land managers, and policy makers are looking for tools that are capable of quantifying N loading rates under conventional or alternative management conditions. Process-based models have been recognized as powerful tools to meet the challenge. As an agroecosystem model, DNDC has been widely used in China to predict crop yields, soil C sequestration, and greenhouse gas emissions with encouraging results [e.g., *Li et al.*, 2010; *Qiu et al.*, 2009; *Tang et al.*, 2006; *Wang et al.*, 2008; *Zhang et al.*, 2006]. Multiyear efforts had been performed to improve the DNDC model to predict soil N leaching losses, but progress has been slow. The key obstacle is to enable the biogeochemical model to simulate horizontal overland flows. *Cui et al.* [2005] attempted to link DNDC to MIKE SHE. This approach required intense coding and memory management, and led to unwieldy information exchange between the hydrologic and biogeochemical algorithms. To explore new strategies, we directly embedded the two fundamental hydrological features, the SCS curve and the MUSLE functions, into DNDC. This innovation has converted DNDC from a one-dimensional to a two-dimensional simulator to include both the vertical and horizontal water and N flows. In the revised model, the new embedded hydrologic processes and other existed algorithms can exchange data at a daily time step, which should improves the model's predictive capacity of N losses in comparison with the approach adopted by *Cui et al.* [2005]. Several hydrologic input parameters are required to run the revised DNDC. The new input data of landform slope, slope length, surface roughness, and other spatially differentiated hydrologic drivers can be derived from topographic maps or digital elevation model (DEM) data with general geographic information system (GIS) processing tools. In this study, we tested the revised DNDC with validations against observations, sensitivity analysis, and Monte Carlo uncertainty analysis. Results from these tests indicate the revised model has normal behaviors in comparison with the observations from the tested site and reports from other researchers. The uncertainty analysis illustrates that possible variance in the input parameters could introduce high potential uncertainties; however, the baseline-simulated results are within the ranges of Monte Carlo simulations and comparable with the means across all Monte Carlo simulations. The attempt reported in this paper demonstrates that it is feasible and effective for improving model prediction on N losses by incorporating basic hydrological features into model framework.

[29] Several researchers reported that the original version of DNDC overestimated soil drainage flows due to the weak capacity of modeling the surface runoff flow [*Kiese et al.*, 2005; *Tonitto et al.*, 2010]. We believe this shortcoming has been improved by the modifications reported in the paper. The validation tests with the revised DNDC demonstrate that the increase in the surface runoff flow did effectively reduce the subsurface leaching flux based upon the water mass balance. As these modifications help to integrate the water and N processes in the DNDC, they should also improve DNDC's predictions on N gas fluxes. A set of hydrologic models, such as MIKE SHE [*Refsgaard and Storm*, 1995], RHESSys [*Band et al.*, 2001; *Tague and Band*, 2001, 2004], SWAT [*Arnold et al.*, 1998; *Neitsch et al.*, 2001; *Saleh et al.*, 2000], and HSPF [*Bicknell et al.*, 1997], tried to incorporate N biogeochemistry in their frameworks to evaluate and predict N dynamic at the watershed scale. These models have been widely applied to simulate N loading from watersheds. Comparison between field measurements and modeled results in their previous applications demonstrated that hydrology-based models usually successfully predicated stream flow, but predicted N loading less accurately, highlighting the difficulty in simulating complex N dynamics of these models [e.g., *Band et al.*, 2001; *Hu et al.*, 2007; *Saleh and Du*, 2004; *Silgram et al.*, 2009; *Yuan et al.*, 2003]. Those applications implied that it is necessary to

include both detailed hydrologic and biogeochemical processes for a model to accurately predict N loading. In comparison with hydrology-based models, the DNDC is relative weak in describing watershed hydrology since it was developed as a site or field-scale model. However, the revised DNDC has the advantage of having long-term tested and relative detailed N processes embedded in the model, which is valuable for the simulation of N loss considering the complexity and tremendous variability of N dynamic.

[30] The integration of biogeochemical models with hydrologic processes is a very interdisciplinary effort. The study reported here is only one attempt in our research agenda. Encouraged by the preliminary results, we will next try to apply the revised DNDC to more watersheds, which will provide us with additional feedback about how to generalize the hydrologic parameters based on the existing DEM data on various spatial scales. More accurate parameterization may also helpful for improving the model's performance on prediction of N losses. For instance, because of the dynamic change of vegetation coverage, the value of soil surface cover and management factor in the MUSLE should varies across different crop-growth stages, although it has been simplified to one value during the entire crop season in most cases [e.g., *Neitsch et al.*, 2001; *Donald et al.*, 2003]. This simplification may hinder the prediction of sediment yield, and subsequently of N losses. Thus, the variance of this parameter across different crop-growth stages should be tested in the future. In addition, to correctly estimate N loadings from the nonpoint agricultural sources to lakes, reservoirs or estuaries, the fate of N in the streams, rivers or other water bodies cannot be ignored. Aquatic biogeochemistry of N and other nutrients will be scheduled in our modeling studies to meet this challenge.

Appendix A

[31] SCS and MUSLE-related equations incorporated in DNDC are as follows:

[32] Surface runoff

$$\begin{array}{ll} Q = (P - Ia)^2/(P + S - Ia) & P > Ia \\ Q = 0 & P \leq Ia \end{array} \tag{A1}$$

$$Ia = 0.2 \cdot S \tag{A2}$$

[33] Retention factor

$$S = (25400/CN) - 254 \tag{A3}$$

[34] Curve number in dry moisture (wilting point) condition

$$\begin{aligned} CN_1 = {} & CN_2 - 20 \cdot (100 - CN_2) \\ & /\{100 - CN_2 + \exp[2.533 - 0.0636 \cdot (100 - CN_2)]\} \end{aligned} \tag{A4}$$

[35] Curve number in wet moisture (field capacity) condition

$$CN_3 = CN_2 \cdot \exp[0.00673 \cdot (100 - CN_2)] \tag{A5}$$

[36] Curve number in average moisture condition adjusted for slope

$$CN_{2s} = (CN_3 - CN_2)/3 \cdot [1 - 2 \cdot \exp(-13.68 \cdot slp)] + CN_2 \tag{A6}$$

[37] Retention parameter varying with the soil water content

$$S = S_{\max} \cdot \{1 - SW/[SW + \exp(w_1 - w_2 \cdot SW)]\} \tag{A7}$$

[38] The first shape coefficient

$$w_1 = \ln\left[FC/\left(1 - S_3 \cdot S_{\max}^{-1}\right) - FC\right] + w_2 \cdot FC \tag{A8}$$

[39] The second shape coefficient

$$\begin{aligned} w_2 = {} & \left\{\ln\left[FC/\left(1 - S_3 \cdot S_{\max}^{-1}\right) - FC\right]\right. \\ & \left. - \ln\left[SAT/\left(1 - 2.54 \cdot S_{\max}^{-1}\right) - SAT\right]\right\}/(SAT - FC) \end{aligned} \tag{A9}$$

[40] Retention parameter adjusted in frozen condition

$$S_{frz} = S_{\max} \cdot [1 - \exp(-0.000862 \cdot S)] \tag{A10}$$

[41] Sediment loading

$$sed = 11.8 \cdot \left(q_{peak} \cdot Q \cdot A\right)^{0.56} \cdot K \cdot LS \cdot C \cdot P_s \cdot R \tag{A11}$$

[42] Peak runoff rate

$$q_{peak} = a_{tc} \cdot Q \cdot A/360 \cdot t_{conc} \tag{A12}$$

[43] Fraction of rain falling in the time of concentration

$$a_{tc} = 1 - \exp[2 \cdot t_{conc} \cdot \ln(1 - a_{0.5})] \tag{A13}$$

[44] Time of concentration

$$t_{conc} = t_{ov} + t_{ch} \tag{A14}$$

[45] Time of concentration for overland flow

$$t_{ov} = L_{slp}^{0.6} \cdot n^{0.6}/\left(18 \cdot slp^{0.3}\right) \tag{A15}$$

[46] Time of concentration for channel flow

$$t_{ch} = 0.62 \cdot L \cdot n^{0.75}/\left(A^{0.125} \cdot slp_{ch}^{0.375}\right) \tag{A16}$$

[47] Soil erodibility factor

$$K = f_{csand} \cdot f_{cl-si} \cdot f_{orgc} \cdot f_{hisand} \tag{A17}$$

$$f_{csand} = \{0.2 + 0.3 \cdot \exp[-0.256 \cdot m_s \cdot (1 - m_{silt}/100)]\} \tag{A18}$$

$$f_{cl-si} = [m_{silt}/(m_c + m_{silt})]^{0.3} \tag{A19}$$

$$f_{orgc} = \{1 - 0.25 \cdot orgC/[orgC + \exp(3.72 - 2.95 \cdot orgC)]\} \quad \text{(A20)}$$

$$f_{hisand} = 1 - 0.7 \cdot (1 - m_s/100)/\{(1 - m_s/100) + \exp[-5.51 + 22.9 \cdot (1 - m_s/100)]\} \quad \text{(A21)}$$

[48] Topographic factor

$$LS = \left(L_{slp}/22.1\right)^m \cdot \left[65.41 \cdot \sin^2(\theta) + 4.56 \cdot \sin(\theta) + 0.065\right] \quad \text{(A22)}$$

$$m = 0.6 \cdot [1 - \exp(-35.835 \cdot slp)] \quad \text{(A23)}$$

$$slp = \tan(\theta) \quad \text{(A24)}$$

[49] Coarse fragment factor

$$R = \exp(-0.053 \cdot rock) \quad \text{(A25)}$$

[50] Sediment carbon transported by surface runoff

$$SedC = 0.001 \cdot conc_{sedC} \cdot sed/A \cdot \varepsilon_{sedC} \quad \text{(A26)}$$

[51] Sediment nitrogen transported by surface runoff

$$SedN = 0.001 \cdot conc_{sedN} \cdot sed/A \cdot \varepsilon_{sedN} \quad \text{(A27)}$$

[52] Enrichment ration

$$\varepsilon = 0.78 \cdot (conc_{sed})^{-0.2468} \quad \text{(A28)}$$

[53] See the notation section for definitions of variables.

Notation

- A plot or hydrology responsibility unit area, ha.
- BD average soil bulk density of the whole profile, g/cm^3.
- C cover and management factor.
- CN curve number.
- CN_1 curve number in dry moisture (wilting point) condition.
- CN_2 curve number in average moisture condition.
- CN_{2S} curve number in average moisture condition adjusted for slope.
- CN_3 curve number in wet moisture (field capacity) condition.
- $conc_{sed}$ concentration of sediment in surface runoff, Mg sed/m^3 H_2O.
- $conc_{sedC}$ concentration of the sediment carbon in the surface soil, g C/tonne soil.
- $conc_{sedN}$ concentration of the sediment nitrogen in the surface soil, g N/tonne soil.
- FC water content in soil profile at field capacity, mm H_2O.
- Ia initial abstractions including soil surface water storage, interception, and infiltration prior to the occurrence of surface runoff, mm H_2O.
- K soil erodibility factor.
- L channel length from the most distant point to the outlet, km.
- L_{slp} plot or subbasin slope length, m.
- LS topographic factor.
- M exponential parameter in LS factor calculation.
- m_c percent soil clay content (<0.002 mm diameter particles).
- m_s percent soil sand content.
- m_{silt} percent soil silt content (0.002–0.05 mm diameter particles).
- n Manning's roughness coefficient for the plot or channel.
- P amount of rainfall on a given day, mm H_2O.
- P_s soil conservation practice factor.
- Q surface runoff on a given day, mm H_2O.
- q_{peak} peak runoff rate, m^3/s.
- R soil coarse fragment factor.
- $rock$ percent rock in soil layer, %.
- S retention parameter in SCS curve number equation, mm.
- S_3 retention parameter in wet moisture condition, mm.
- S_{frz} retention parameter adjusted in frozen condition, mm.
- $S_{\max}$ maximum retention parameter on any given day, mm.
- SAT amount of water in the soil profile when completely saturated, mm H_2O.
- sed sediment yields on a given day, metric tons.
- slp average slope of plot or subbasin, m/m.
- SW amount of water in the soil profile, mm H_2O.
- t_{ch} time of concentration for channel flow, h.
- t_{conc} time of concentration for a plot or subbasin, h.
- t_{ov} time of concentration for overland flow, h.
- w_1 shape coefficient in equation adjusting retention parameter based on soil water content.
- w_2 shape coefficient in equation adjusting retention parameter based on soil moisture content.
- $a_{0.5}$ fraction of daily rainfall occurring in the half-hour with highest rainfall intensity.
- a_{tc} fraction of daily rainfall occurring during the time of concentration.
- θ angle of the slope, degree.
- ε enrichment ratio.

[54] **Acknowledgments.** This study was supported by the Ministry of Agriculture of China (200803036), the National Natural Science Foundation of China (40571093, 41021004), and the European Union (NitroEurope IP 017841). The participation of Changsheng Li in the study was supported by the NASA Terrestrial Ecology sponsored project "Modeling impacts of climate change on carbon dynamics in northern high latitude wetlands" (08-TE08-13).

References

Arnold, J. G., R. Srinivasan, R. S. Muttiah, and J. R. Williams (1998), Large area hydrologic modeling and assessment part I: Model development, *J. Am. Water Resour. Assoc.*, *34*(1), 73–89, doi:10.1111/j.1752-1688.1998.tb05961.x.

Band, L. E., C. L. Tague, P. Groffman, and K. Belt (2001), Forest ecosystem processes at the watershed scale: Hydrologic and ecological controls of nitrogen export, *Hydrol. Process.*, *15*, 2013–2028, doi:10.1002/hyp.253.

Bicknell, B. R., J. C. Imhoff, J. L. Kittle Jr., A. S. Donigian Jr., and R. C. Johanson (1997), Hydrologic simulation program—FORTRAN user's manual for release 11, U.S. Environ. Prot. Agency—Atlanta, Ga.

Boyer, E. W., R. B. Alexander, W. J. Parton, C. Li, K. Butterbach-Bahl, S. D. Donner, R. W. Skaggs, and S. J. Delgrosso (2006), Modeling denitrification in terrestrial and aquatic ecosystems at regional scales, *Ecol. Appl.*, *16*(6), 2123–2142, doi:10.1890/1051-0761(2006)016[2123:MDITAA]2.0.CO;2.

Carpenter, S. R., N. F. Caraco, D. L. Correll, R. W. Howarth, A. N. Sharpley, and V. H. Smith (1998), Nonpoint pollution of surface waters with phosphors and nitrogen, *Ecol. Appl.*, *8*(3), 559–568, doi:10.1890/1051-0761(1998)008[0559:NPOSWW]2.0.CO;2.

Cassman, K. G., A. Dobermann, and D. T. Walters (2002), Agroecosystems, nitrogen-use efficiency, and nitrogen management, *Ambio*, *31*(2), 132–140.

Cui, J., C. Li, G. Sun, and C. Trettin (2005), Linkage of MIKE SHE to Wetland-DNDC for carbon budgeting and anaerobic biogeochemistry simulation, *Biogeochemistry*, *72*(2), 147–167, doi:10.1007/s10533-004-0367-8.

Deng, L., D. B. Hou, C. Q. Wang, S. R. Zhang, and J. G. Xia (2003), Study on characteristics of erodibility of natural soil and non-irrigated soil of Sichuan (in Chinese), *Soil Water Conserv. China*, *7*, 23–25.

Donald, G., G. Ghekiere, W. Schiettecatte, and I. Rottiers (2003), Assessment of USLE cover-management C-factors for 40 crop rotation systems on arable farms in the kemmelbeek watershed, Belgium, *Soil Tillage Res.*, *74*, 47–53, doi:10.1016/S0167-1987(03)00092-8.

Galloway, J. N., J. D. Aber, J. W. Erisman, S. P. Seitzinger, R. H. Howarth, E. B. Cowling, and B. J. Cosby (2003), The nitrogen cascade, *BioScience*, *53*(4), 341–356, doi:10.1641/0006-3568(2003)053[0341:TNC]2.0.CO;2.

Gao, Y., B. Zhu, Y. C. Miao, and J. Z. Zhang (2006), Application of SCS model to estimate the volume of rainfall runoff in sloping field of purple soil (in Chinese), *Chin. Agric, Sci. Bull.*, *22*(11), 396–400.

Helton, J. C., and F. J. Davis (2003), Latin hypercube sampling and the propagation of uncertainty in analysis of complex systems, *Reliab. Eng. Syst. Saf.*, *81*, 23–69, doi:10.1016/S0951-8320(03)00058-9.

Hu, X., G. F. McIsaac, M. B. David, and C. A. L. Louwers (2007), Modeling riverine nitrate export from an east-central Illinois watershed using SWAT, *J. Environ. Qual.*, *36*, 996–1005, doi:10.2134/jeq2006.0228.

Jaynes, D. B., T. S. Colvin, D. L. Karlen, C. A. Cambardella, and D. W. Meek (2001), Nitrate loss in subsurface drainage as affected by nitrogen fertilizer rate, *J. Environ. Qual.*, *30*, 1305–1314, doi:10.2134/jeq2001.3041305x.

Karlen, D. L. (1998), Field-scale nitrogen balances associated with long-term continuous corn production, *Agron. J.*, *90*(5), 644–650, doi:10.2134/agronj1998.00021962009000050013x.

Kiese, R., C. Li, D. W. Hilbert, H. Papen, and K. Butterbach-Bahl (2005), Regional application of PnET-N-DNDC for estimating the N_2O source strength of tropical rainforests in the wet tropics of Australia, *Global Change Biol.*, *11*(1), 128–144, doi:10.1111/j.1365-2486.2004.00873.x.

Kimura, S. D., R. Hatano, and M. Okazaki (2009), Characteristics and issues related to regional-scale modeling of nitrogen flows, *Soil Sci. Plant Nutr.*, *55*(1), 1–12, doi:10.1111/j.1747-0765.2008.00353.x.

Li, C. (2000), Modeling trace gas emissions from agricultural ecosystems, *Nutr. Cycl. Agroecosyst.*, *58*(1–3), 259–276, doi:10.1023/A:1009859006242.

Li, C., S. Frolking, and T. A. Frolking (1992a), A model of nitrous oxide evolution from soil driven by rainfall events: 1. Model structure and sensitivity, *J. Geophys. Res.*, *97*(D9), 9759–9776.

Li, C., S. Frolking, and T. A. Frolking (1992b), A model of nitrous oxide evolution from soil driven by rainfall events: 2. Model applications, *J. Geophys. Res.*, *97*(D9), 9777–9783.

Li, C., S. Frolking, and R. Harriss (1994), Modeling carbon biogeochemistry in agricultural soils, *Global Biogeochem. Cycles*, *8*, 237–254, doi:10.1029/94GB00767.

Li, C., V. Narayanan, and R. Harriss (1996), Model estimates of nitrous oxide emissions from agricultural lands in United States, *Global Biogeochem. Cycles*, *10*, 297–306, doi:10.1029/96GB00470.

Li, C., N. Farahbakhshazad, D. B. Jaynes, D. L. Dinnes, W. Salas, and D. McLaughin (2006), Modeling nitrate leaching with a biogeochemical model modified based on observations in a row-crop field in Iowa, *Ecol. Modell.*, *196*, 116–130, doi:10.1016/j.ecolmodel.2006.02.007.

Li, H., J. Qiu, L. Wang, H. Tang, C. Li, and E. Van Ranst (2010), Modelling impacts of alternative farming management practices on greenhouse gas emissions from a winter wheat-maize rotation system in China, *Agric. Ecosyst. Environ.*, *135*, 24–33, doi:10.1016/j.agee.2009.08.003.

McElroy, A. D., S. Y. Chiu, J. W. Nebgen, A. Aleti, and F. W. Bennett (1976), Loading functions for assessment of water pollution from non-point sources, Midwest Res. Inst., Kansas City, Mo.

Miehle, P., S. j. Liversley, C. Li, P. M. Feikema, M. A. Adams, and S. K. Arndt (2006), Quantifying uncertainty from large-scale model predictions of forest carbon dynamics, *Global Change Biol.*, *12*(8), 1421–1434, doi:10.1111/j.1365-2486.2006.01176.x.

Mockus, V. (1972), Hydrology, in *National Engineering Handbook*, U.S. Dep. of Agric., Washington, D. C.

Moriasi, D. N., J. G. Arnold, M. W. Van Liew, R. L. Bingner, R. D. Harmel, and T. L. Veith (2007), Model evaluation guidelines for systematic quantification of accuracy in watershed simulations, *Trans. ASABE*, *50*(3), 885–900.

Nash, J. E., and J. V. Sutcliffe (1970), River flow forecasting through conceptual models part I: A discussion of principles, *J. Hydrol.*, *10*(3), 282–290, doi:10.1016/0022-1694(70)90255-6.

Nearing, M. A., L. Deer-Ascough, and J. M. Laflen (1990), Sensitivity analysis of the WEPP hillslope profile erosion model, *Trans. ASAE*, *33*(3), 839–849.

Neitsch, S. L., J. G. Arnold, J. R. Kiniry, J. R. Williams, and K. W. King (2001), Soil and water assessment tool theoretical documentation, Blackland Res. Cent., Tex. Agric. Exp. Stn., Temple.

Ng Kee Kwong, K. F., A. Bholah, L. Volcy, and K. Pynee (2002), Nitrogen and phosphorus transport by surface runoff from a silty clay loam soil under sugarcane in the humid tropical environment of Mauritius, *Agric. Ecosyst. Environ.*, *91*(1–3), 147–157, doi:10.1016/S0167-8809(01)00237-7.

Novotny, V., and H. Olem (1994), *Water Quality: Prevention, Identification, and Management of Diffuse Pollution*, Van Nostrand Reinhold, New York.

Qiu, J., C. Li, L. Wang, H. Tang, H. Li, and E. Van Ranst (2009), Modeling impacts of carbon sequestration on net greenhouse gas emissions from agricultural soils in China, *Global Biogeochem. Cycles*, *23*, GB1007, doi:10.1029/2008GB003180.

Rabalais, N. N. (2002), Nitrogen in aquatic ecosystems, *Ambio*, *31*(2), 102–112.

Refsgaard, J. C., and B. Storm (1995), MIKE SHE, in *Computer Models of Watershed Hydrology*, pp. 809–846, Water Resour. Publ., Highlands Ranch, Colo.

Saleh, A., and B. Du (2004), Evaluation of SWAT and HSPF within basin programs for the upper North Bosque River watershed in central Texas, *Trans. ASAE*, *47*(4), 1039–1049.

Saleh, A., J. G. Arnold, P. W. Gassman, L. M. Hauck, W. D. Rosenthal, J. R. Williams, and A. M. S. McFarland (2000), Application of SWAT for the upper North Bosque River watershed, *Trans. ASAE*, *43*(5), 1077–1087.

Schlesinger, W. H., A. D. Abrahams, A. J. Parsons, and J. Wainwright (1999), Nutrient losses in runoff from grassland and shrubland habitats in southern New Mexico: I. Rainfall simulation experiments, *Biogeochemistry*, *45*(1), 21–34, doi:10.1007/BF00992871.

Seitzinger, S. (2008), Nitrogen cycle - Out of reach, *Nature*, *452*, 162–163, doi:10.1038/452162a.

Seitzinger, S., J. A. Harrison, E. Dumont, A. H. W. Beusen, and A. F. Bowman (2005), Source and delivery of carbon, nitrogen and phosphorous to the coastal zone: An overview of Global Nutrient Export from Watershed (NEWS) models and their application, *Global Biogeochem. Cycles*, *19*, GB4S01, doi:10.1029/2005GB002606.

Shi, X. Z., D. S. Yu, and T. Y. Xing (1997), Soil erodibility factor K as studied using field plots in subtropical China (in Chinese), *Acta Pedol. Sin.*, *34*(4), 399–405.

Silgram, M., et al. (2009), Subannual models for catchment management: Evaluating model performance on three European catchments, *J. Environ. Monit.*, *11*, 536–539, doi:10.1039/b823250d.

Soil Conservation Service (SCS) (1986), Urban hydrology for small watershed, Eng. Div., U.S. Dep. of Agric., Washington, D. C.

Tague, C. L., and L. E. Band (2001), Evaluating explicit and implicit routing for watershed hydro-ecological models of forest hydrology at the small catchment scale, *Hydrol. Process.*, *15*, 1415–1439, doi:10.1002/hyp.171.

Tague, C. L., and L. E. Band (2004), RHESSys: Regional Hydro-ecologic Simulation System—An object-oriented approach to spatially distributed modeling of carbon, water, and nutrient cycling, *Earth Interact.*, *8*(19), 1–40, doi:10.1175/1087-3562(2004)8<1:RRHSSO>2.0.CO;2.

Tang, H., J. Qiu, E. Van Ranst, and C. Li (2006), Estimations of soil organic carbon storage in cropland of China based on DNDC model, *Geoderma*, *134*, 200–206, doi:10.1016/j.geoderma.2005.10.005.

Tilman, D., J. Fargione, B. Wolff, C. D'Antonio, A. Dobson, R. Howarth, D. Schindler, W. H. Schlesinger, D. Simberloff, and D. Swackhamer (2001), Forecasting agriculturally driven global environmental change, *Science*, *292*, 281–284, doi:10.1126/science.1057544.

Tonitto, C., M. B. David, L. E. Drinkwater, and C. Li (2007), Application of the DNDC model to tile-drained Illinois agroecosystems: Model calibration, validation, and uncertainty analysis, *Nutr. Cycl. Agroecosyst.*, *78*(1), 51–63, doi:10.1007/s10705-006-9076-0.

Tonitto, C., C. Li, R. Seidel, and L. E. Drinkwater (2010), Application of the DNDC model to the Rodale Institute Farming Systems Trial: Challenges for the validation of drainage and nitrate leaching in agroecosystem models, *Nutr. Cycl. Agroecosyst.*, doi:10.1007/s10705-010-9354-8.

Walker, S. E., J. K. Mitchell, M. C. Hirschi, and K. E. Johnsen (2000), Sensitivity analysis of the root zone water quality model, *Trans. ASAE*, *43*(4), 841–846.

Wang, L., J. Qiu, H. Tang, H. Li, C. Li, and E. Van Ranst (2008), Impacts of farming management alternatives on soil organic carbon dynamics across major agricultural regions in China, *Geoderma*, *147*, 47–55, doi:10.1016/j.geoderma.2008.07.009.

Wang, T., B. Zhu, M. R. Gao, T. P. Xu, and F. H. Kuang (2006), Nitrate pollution of groundwater in a typical small watershed in the central Sichuan hilly region (in Chinese), *J. Ecol. Rural Environ*, *22*, 84–87.

White, K. L., and I. Chaubey (2005), Sensitivity analysis, calibration, and validations for a multisite and multivariable SWAT model, *J. Am. Water Resour. Assoc.*, *41*(5), 1077–1089.

Williams, J. R. (1975), Sediment-yield prediction with universal equation using runoff energy factor, in *Present and Prospective Technology for Predicting Sediment Yields and Sources*, pp. 244–252, U.S. Dep. of Agric., Washington, D. C.

Williams, J. R. (1995), The EPIC model, in *Computer Models of Watershed Hydrology*, pp. 909–1000, Water Resour. Publ., Highlands Ranch, Colo.

Williams, J. R., and R. W. J. Hann (1978), Optimal operation of large agricultural watersheds with water quality constraints, Tex. Water Resour. Inst., Tex. A&M Univ., College Station.

Wischmeier, W. H., and D. D. Smith (1978), Predicting rainfall erosion losses: A guide to conservation planning, U.S. Dep. of Agric., Washington, D. C.

Yan, H. M., J. Y. Liu, and M. K. Cao (2007), Spatial pattern and topographic control of China's agricultural productivity variability, *Acta Geogr. Sin.*, *62*(2), 171–180.

Yuan, Y. P., B. L. Bingner, and R. A. Rebich (2003), Evaluation of AnnAGNPS nitrogen loading in an agricultural watershed, *J. Am. Water Resour. Assoc.*, *39*(2), 457–466.

Zhang, F., C. Li, Z. Wang, and H. Wu (2006), Modeling impacts of management alternatives on soil carbon storage of farmland in northwest China, *Biogeosciences*, *3*, 451–466, doi:10.5194/bg-3-451-2006.

Zhang, Y., B. Y. Liu, P. J. Shi, and Z. S. Jiang (2001), Crop cover factor estimating for soil loss prediction (in Chinese), *Acta Ecol. Sin.*, *21*(7), 1050–1056.

Zhang, Y., C. Li, C. C. Trettin, H. Li, and G. Sun (2002), An integrated model of soil, hydrology and vegetation for carbon dynamics in wetland ecosystems, *Global Biogeochem. Cycles*, *16*(4), 1061, doi:10.1029/2001GB001838.

Zhu, B., T. Wang, T. P. Xu, F. H. Kuang, Z. X. Luo, and Y. Gao (2006), Non-point source nitrogen movement and its environmental effects in a small watershed in hilly area of purple soil (in Chinese), *J. Mt. Sci.*, *24*, 601–606.

Zhu, B., T. Wang, F. H. Kuang, T. P. Xu, and Z. X. Luo (2008), Characteristics of nitrate leaching from sloping cropland of purple soil (in Chinese), *Acta Sci. Circum.*, *28*, 525–533.

Zhu, B., T. Wang, F. H. Kuang, Z. X. Luo, J. L. Tang, and T. P. Xu (2009), Measurements of nitrate leaching from a hillslope cropland in the Central Sichuan Basin, China, *Soil Sci. Soc. Am. J.*, *73*(4), 1419–1426, doi:10.2136/sssaj2008.0259.

Zhu, Z., D. Noese, and B. Sun (2006), Policy for reducing non-point pollution from crop production in China, China Environ. Sci. Press, Beijing.

J. Deng, X. Zheng, and Z. Zhou, State Key Laboratory of Atmospheric Boundary Layer Physics and Atmospheric Chemistry, Institute of Atmospheric Physics, Chinese Academy of Sciences, Beijing 100029, China. (zhouzx@mail.iap.ac.cn)

C. Li, Complex Systems Research Center, Institute for the Study of Earth, Oceans, and Space, University of New Hampshire, 39 College Rd., Durham, NH 03824, USA.

J. Tang, T. Wang, and B. Zhu, Institute of Mountain Hazards and Environment, Chinese Academy of Sciences, Chengdu 610041, China.